SPECIAL SECTION: ORIGINAL ARTICLE

New developments in mode-water research: Dynamic and climatic effects

The role of meso-scale eddies in mixed layer deepening and mode water formation in the western North Pacific

Shinya Kouketsu · Hiroyuki Tomita · Eitarou Oka · Shigeki Hosoda · Taiyo Kobayashi · Kanako Sato

Abstract Distributions of mixed layer depths around the centers of anti-cyclonic and cyclonic eddies in the North Pacific Ocean were composited by using satellite-derived sea surface height anomaly data and Argo profiling float data. The composite distributions showed that in late winter, deeper mixed layers were more (less) frequently observed inside the cores of the anti-cyclonic (cyclonic) eddies than outside. This relationship was the clearest in the region of 140°E–160°W and 35°N–40°N, where the temperature and salinity of the deep mixed layers were similar to those of the lighter variety of central mode water (L-CMW). A simple one-dimensional bulk mixed layer model showed that both strong sea-surface heat and momentum fluxes and weak preexisting stratification contributed to formation of the deep mixed layer. These conditions were associated with the anti-cyclonic eddies, suggesting that these eddies are important in the formation of mode waters, particularly L-CMW.

Keywords Mixed layer · Mode water · Meso-scale eddy · Sea-surface flux

S. Kouketsu (✉) · H. Tomita · S. Hosoda · T. Kobayashi · K. Sato
Research Institute for Global Change,
Japan Agency for Marine-Earth Science and Technology,
2-15 Natsushima-cho, Yokosuka 237-0061, Japan
e-mail: skouketsu@jamstec.go.jp

H. Tomita
e-mail: tomitah@jamstec.go.jp

S. Hosoda
e-mail: hosodas@jamstec.go.jp

T. Kobayashi
e-mail: taiyok@jamstec.go.jp

K. Sato
e-mail: k_sato@jamstec.go.jp

E. Oka
Atmosphere and Ocean Research Institute,
The University of Tokyo, Kashiwa, Japan
e-mail: eoka@aori.u-tokyo.ac.jp

1 Introduction

Ocean surface mixed layers, which are the layers at the ocean surface with vertically uniform water properties, develop as a result of momentum and buoyancy forcing, especially in winter. Because heat, freshwater and chemical components (e.g., CO_2) are exchanged between the ocean and the atmosphere through the mixed layers (Takahashi et al. 2009; Hosoda et al. 2010), mixed layer depths (MLDs) and properties are strongly related to climate and environmental variability. Furthermore, deep mixed layers that develop in winter are separated from surface forcing by surface re-stratification, mainly because of heating in spring, and remain in the subsurface as the frequently observed thick, vertically homogeneous layers called "mode waters" (Hanawa and Talley 2001). In association with mode water formation and subduction, the heat, freshwater, and chemical components that are exchanged with the atmosphere and the materials produced by the biological processes near the sea surface are transported to the subsurface layers in the ocean. The part of mode waters remains under the seasonal thermocline, and is entrained again in the deep mixed layer during the next winter. This process affects the late-winter sea surface temperature anomaly in some regions (Hanawa and Sugimoto 2004; Sugimoto and Hanawa 2005). The other part is subducted to the permanent pycnocline. The mode water formation and subduction are crucially involved in long-term

subsurface temperature or other environmental changes (Talley and Raymer 1982; Deser et al. 1996; Emerson et al. 2004), and might have an important effect on decadal climate variability (Latif and Barnett 1994; Gu and Philander 1997).

On the western side of the North Pacific Ocean, subtropical mode water (STMW; Masuzawa 1969), central mode water (CMW; Nakamura 1996; Suga et al. 1997), and transition region mode water (TRMW; Saito et al. 2007) are frequently observed as the subsurface vertically homogeneous layers. STMW and CMW are formed as deep winter mixed layers in the region south and north, respectively, of the Kuroshio Extension (Suga et al. 2004), and TRMW is formed south of the subarctic front (Saito et al. 2007). Investigations into the formation and seasonal evolution of the deep mixed layers in the mode-water formation regions have mainly used climatology or spatially sparse observations (Suga et al. 2004; Ohno et al. 2009). Recently, profiling float data became available for the global ocean (Roemmich 2001), and the distribution and structure of the deep mixed layers and mode waters have been investigated in more detail (Oka et al. 2011; Toyama and Suga 2010).

Oka et al. (2011) showed the detailed distribution of the late-winter deep mixed layer in the North Pacific and its relationships with mode waters. They divided the mode waters into four types—STMW, the lighter and denser varieties of CMW (L-CMW and D-CMW; Tsujino and Yasuda 2004; Oka and Suga 2005), and TRMW—by using the temperature and salinity relationships of deep mixed layers as observed by profiling floats. They found that L-CMW, D-CMW, and TRMW become lighter to the east and subduct into the permanent thermocline from the eastern part of the formation region where the deep mixed layers were observed.

In the western North Pacific, the warm (cold) and saline (fresh) anti-cyclonic (cyclonic) eddies known as warm-core (cold-core) rings, which originate from the Kuroshio Extension, are frequently observed (Mizuno and White 1983; Kawamura et al. 1986; Itoh and Yasuda 2010), and their relatively weak (strong) preexisting stratification accompanied by deep (shallow) thermocline can create favorable (unfavorable) conditions for mixed-layer deepening. The spatial changes in preexisting stratification structure associated with the eddies may cause small-scale spatial changes in MLDs. Indeed, there is small-scale spatial variability in the mixed-layer distribution map of Oka et al. (2011), and deep mixed layers have frequently been observed in the ridges and anti-cyclonic eddies along the Kuroshio Extension (Uehara et al. 2003; Qiu et al. 2006; Oka 2009).

Furthermore, small-scale spatial changes in wind and buoyancy corresponding to ocean fronts or eddies have been detected (Nonaka and Xie 2003; White and Annis 2003; Tokinaga et al. 2006), and these changes are important in the distribution of rainfall near oceanic fronts (Minobe et al. 2008; Tokinaga et al. 2010). As the mixed layer develops as a result of momentum and buoyancy fluxes from the atmosphere, spatial changes in fluxes can also contribute to changes in MLDs with the distances from the eddy core. The earlier studies did not describe in detail the effects of small-scale flux variability on the ocean mixed layer; however, more recent studies (Tomita et al. in preparation) have reported that small-scale spatial changes in the forcings across the subarctic front can contribute to those in MLDs.

Recent high-resolution numerical experiments have shown the importance of eddies in the formation and transport of mode waters (especially for STMW) (Tsujino and Yasuda 2004; Rainville et al. 2007; Nishikawa et al. 2010). There have also been many observational descriptions of deep mixed layers and mode water formation in the cores of eddies for the STMW formation area (Uehara et al. 2003; Qiu et al. 2006; Oka 2009), but there were few for the whole western North Pacific. Here we describe the relationships between the late-winter deep mixed layer and meso-scale eddies in the whole western North Pacific and clarify the effects of changes in ocean stratification, accompanied by changes in thermocline depths, and of forcing fields associated with eddies on mixed layer development and mode water formation.

2 Data and methods

Gridded sea surface height anomaly (SSHA) data were produced by Segment Sol Multimissions d'Alimétrie d'Orbitographie et de Localization Precise/Data Unification and Altimeter Combination System (Ssalto/Ducas) and distributed by Archiving, Validation and Interpretation of Satellites Oceanographic Data (AVISO) with support from Centre National d'Etudes Spatiales (CNES). The SSHA map provided was a 7-day composite with $\frac{1}{3}° \times \frac{1}{3}°$ grids. Meso-scale eddies were detected by use of the satellite SSHA data and essentially the same methods as in previous studies (Chelton et al. 2007; Itoh and Yasuda 2010), which defined eddies as areas where the Okubo–Weiss parameter W ($= 4\,[(\partial u / \partial x)^2 + (\partial v / \partial x)\,(\partial u / \partial y)]$), calculated from an SSHA map was less than a critical value (Fig. 1). The center of an eddy is defined as a centroid of the SSHA. In tracking the eddies detected in each 7-day composite, we searched for the nearest eddy from the center of an eddy detected on the previous map (7 days earlier) within a set search range. In this study, we set the critical value of the Okubo–Weiss parameter to $-0.2 \times \sigma_W$ to allow for the spatial variability of eddy strength, where σ_W is the

Fig. 1 Sea surface height anomaly (cm) and centers of detected anti-cyclonic (*white circles*) and cyclonic (*black circles*) eddies in the composite of the western North Pacific Ocean for Mar 12, 2008
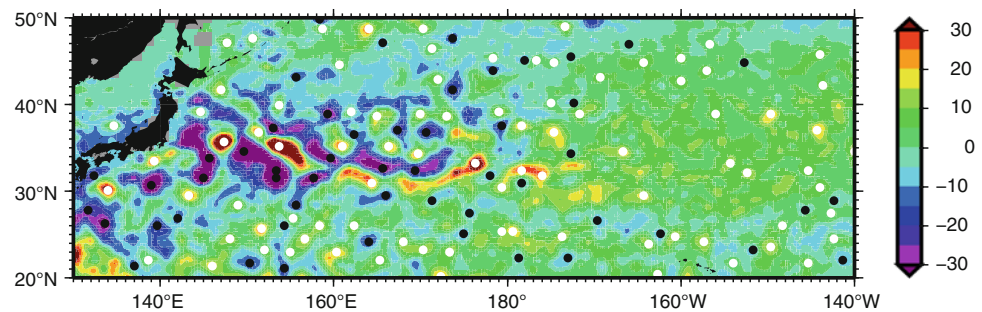
standard deviation of the Okubo–Weiss parameter in a $5° \times 2.5°$ box (longitude $\times$ latitude). The factor of -0.2 was chosen on the basis information presented by Isern-Fontanet et al. (2004), and the resulting critical value east of Japan was similar to that used by Itoh and Yasuda (2010) who investigated meso-scale eddies moving through the same region. The search range for tracking eddies was set to 100 km and we used only eddies that could be tracked for over 4 weeks, as recommended by Itoh and Yasuda (2010).

To determine the MLDs, we used temperature and salinity profiles obtained by Argo profiling floats in the North Pacific from 2002 to 2009. These floats drift at a parking pressure (typically 1000 dbar) and take measurements from an intermediate depth (2000 dbar) to near the sea surface at a preset time interval (10 days). In a typical profile, temperature and salinity are measured at intervals of 5 dbar over the upper 200 dbar, 10–25 dbar from 200 to 1000 dbar, and 50–100 dbar deeper than 1000 dbar. We used real-time quality-controlled float data (Wong et al. 2010) and eliminated questionable profiles, for example those with flagged measurements, by using the same method as Oka et al. (2007). We then interpolated the profile data to 1-dbar intervals by using the Akima spline method (Akima 1970).

MLDs were defined as the depths at which the density was 0.03 kg m^{-3} greater than that at the 10-m depth for each profile (Weller and Plueddemann 1996). Other studies have used vertical temperature differences as the criterion for defining MLDs (de Boyer Montégut et al. 2004), however the difference between MLDs estimated with and without the temperature criterion is not large in the North Pacific (Hosoda et al. 2010). Because large density difference criteria used in previous studies (typically 0.125 kg m^{-3}) are sometimes too large to detect MLDs using Argo float data (Hosoda et al. 2010), we used the small vertical density difference criterion. The mixed layer temperature and salinity were defined as the vertical mean over the obtained MLDs. To make composites, we set four sub regions in the region of 140°E–160°W and 25°N–45°N where almost all of deep mixed layers were observed in the

western North Pacific (Oka et al. 2011). The southernmost region in the four sub regions is 25°N–30°N. The regions 30°N–35°N and 35°N–40°N approximately correspond to the main formation regions of STMW and L-CMW, respectively. In the western and eastern parts of the northernmost region of 40°N–45°N, TRMW and D-CMW are formed (Oka et al. 2011). All MLDs observed in the North Pacific region were arranged in order of their distance from the center of the eddy nearest to each profile. We then made composites of the observed MLDs along the radial direction of the eddies in the sub regions in late winter (February–April), when the mixed layers were the deepest of the year (Oka et al. 2007). In the composites, we show 50-km bin averages along the radial direction with their bootstrapped confidence intervals calculated with the bootstrap sample number of 3000 (Von Storch and Zwiers 1999). Note that all the profiles are divided into two groups: near the anti-cyclonic and cyclonic eddy centers, in this method. In this study, we especially focus on "deep mixed layers" deeper than 150 m in the composites, because the deep mixed layers contribute strongly to the formation of mode waters (Suga et al. 2004; Oka et al. 2011).

To investigate the relationship of the distribution of surface momentum and heat fluxes to the meso-scale eddies in the regions, we used a high-resolution satellite-derived air-sea heat flux dataset that was developed as version 2 of the Japanese ocean flux data sets with use of remote sensing observations (J-OFURO2; Tomita et al. 2010). This dataset provided the daily turbulent heat fluxes at the sea surface on a $0.25° \times 0.25°$ grid from 2002 to 2007. We also used the sea surface temperature data that were used to calculate the turbulent heat fluxes in J-OFURO2.

To quantify the contributions of ocean stratification and the sea-surface fluxes to variations in MLD, we used a bulk one-dimensional mixed layer model, assuming that horizontal advection and diffusion over the mixed-layer thickness is small in the core of meso-scale eddies. In the model, we used the following equations to determine MLD (h_{m}):

$$\frac{\partial h_{\mathrm{m}}}{\partial t} = w_{\mathrm{e}},$$

$$\frac{\partial T_{\mathrm{m}}}{\partial t} = \frac{Q_{\mathrm{net}} - q_d}{\rho_{\mathrm{o}} c h_{\mathrm{m}}} - \frac{\Delta T}{h_{\mathrm{m}}} w_{\mathrm{e}},$$

$$w_{\mathrm{e}} = \frac{C_1 u_*^3 - C_2 B h_{\mathrm{m}}}{\alpha g h \Delta T}, \qquad (1)$$

$$B = \alpha g \frac{Q_{\mathrm{net}} + q_{\mathrm{d}}}{\rho_{\mathrm{o}} c},$$

$$\Delta T \equiv T_{\mathrm{m}} - T(z = -h_{\mathrm{m}} - 20).$$

The coefficients and variables in the equations are summarized in Table 1. The coefficients were set to values similar to those in previous studies (Yasuda et al. 2000; Kako and Kubota 2009). Q_{net} was the sum of the turbulent heat fluxes from J-OFURO2 and the radiative heat fluxes from the National Centers for Environment Prediction (NCEP (NOAA, USA); Kalnay et al. 1996), and u_* was calculated from daily mean momentum fluxes in J-OF-URO2. ΔT was defined as the temperature difference between the mixed layer and 20 m below the base of the mixed layer. To create a composite view near the center of meso-scale eddies, we set the initial stratification structures of 50-km-bin average temperature profiles around the center of eddies to the averages of profiles observed from October to December in 2002–2007. The winter mean (from November to March) momentum and net heat fluxes were also estimated for each 50-km bin along the radial direction of the eddies. Because the winter mean fluxes met the requirements for mixed layer deepening, only the equations for mixed layer deepening (Eq. 1) are used in this study. Using the mean initial stratification and surface

Table 1 Summary of variables and coefficients for a bulk ocean mixed layer model (Eq. 1)

Variable	Description
h_{m}	Mixed layer depth
T_{m}	Mixed layer temperature
w_{e}	Entrainment velocity
u_*	Frictional velocity
B	Net buoyancy flux
C_1	Tuning coefficients (=1.0)
C_2	Tuning coefficients (=0.2)
α	The thermal expansion coefficient of the seawater ($=2.5 \times 10^{-4}\ {}^{\circ-1}$)
g	Gravitational acceleration
ΔT	The temperature difference between the mixed layer and the layer below
Q_{net}	Net surface heat flux
q_{d}	Downward radiative flux at the base of the mixed layer
ρ_{o}	The reference density
c	The specific heat of seawater ($=3.99 \times 10^3\ \mathrm{kg}^{-1}\ \mathrm{J}^{-1}$)

fluxes, we integrated the model from November 15 to March 15 to obtain estimated MLDs.

3 Results

3.1 Relationship between deep mixed layers and meso-scale eddies

The composite analysis revealed that deep mixed layers were more frequently observed in the anti-cyclonic eddies than in the cyclonic eddies in the late winter from 2002 to 2009 (Fig. 2). In the region from 25°N to 30°N, 50-km bin averaged MLDs were approximately 50 m in most of the bins near both the anti-cyclonic and cyclonic eddies, and there was no clear relationship between MLDs and the distance from eddies of either type (Fig. 2a).

From 30°N to 35°N, the MLDs in the anti-cyclonic eddies were deeper than those in the cyclonic eddies, and were deeper (shallower) closer to the core of the anti-cyclonic (cyclonic) eddies (Fig. 2b). The differences between MLDs in the anti-cyclonic and cyclonic eddies were mainly associated with the ridges and troughs of a quasi-stationary meander along the Kuroshio Extension (Mizuno and White 1983; Tatebe and Yasuda 2001), which can be detected as eddies by this method. The deep mixed layers in the anti-cyclonic eddies or the ridges of the meander have been reported previously, and the contribution of the deep mixed layers to the formation of STMW has been shown (Uehara et al. 2003; Qiu et al. 2006; Oka 2009). Although there were clear differences between MLD distributions in the anti-cyclonic and cyclonic eddies, and the bin-averaged MLDs were significantly smaller inside 150 km from the cyclonic eddy center than outside, the differences between MLDs inside and outside of 150 km from the anti-cyclonic eddy center was insignificant in comparison with the 95% confidence intervals for the bin average (Fig. 2b). This region is mostly located south of the Kuroshio Extension, where the preexisting stratification under the seasonal thermocline was relatively weak because of STMW in the subsurface layer. Such large-horizontal-scale distribution of weak preexisting stratification resulted in a deepened mixed layer even away from the core of the anti-cyclonic eddies.

From 35°N to 40°N, differences were evident in the distributions of MLD between inside and outside 100 km from the anti-cyclonic eddy center and between inside 100 km from the anti-cyclonic and cyclonic eddy centers, whereas the difference between inside and outside the cyclonic eddies was not clear in comparison with the 95% confidence intervals (Fig. 2c). Over 70% of all observed MLDs within 50 km of the anti-cyclonic cores were deep MLDs (>150 m), and the bin-averaged MLD was approximately 200 m, whereas the bin-averaged MLDs

Fig. 2 Distributions of mixed layer depths as a function of distance (R) from the center of meso-scale eddies in late winter (from February to April). *Dots* denote observed mixed layers. *Open circles* and *bars* denote the 50-km bin averages and bootstrapped 95% confidence intervals, respectively, of the mixed layer depth. *Solid black bars* denote the ratio of deep mixed layers (>150 m) to all mixed layer observations in the 50-km bins from 2002 to 2009

(a) 25°N–30°N,140°E–160°W

(b) 30°N–35°N,140 °E–160°W

(c) 35°N–40°N,140 °E–160°W

(d) 40°N–45°N,140 °E–160°W
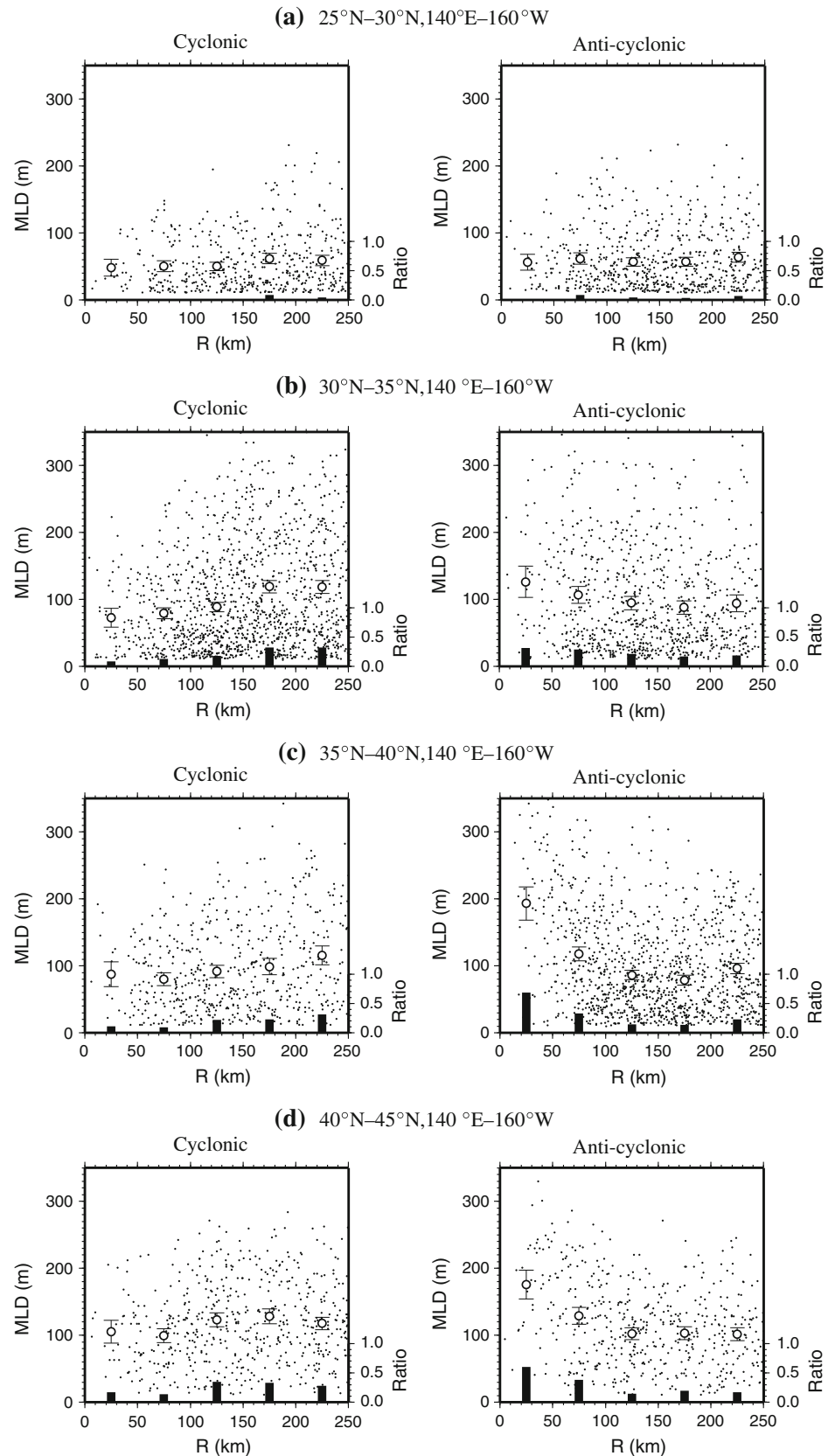
more than 50 km from the core were less than 120 m. In this region, warm and saline anti-cyclonic eddies known as warm-core rings, which originate from the Kuroshio Extension, are frequently observed (Mizuno and White, 1983; Kawamura et al. 1986; Itoh and Yasuda 2010), and their relatively weak preexisting stratification create favorable conditions for mixed-layer deepening. The presence of many eddies with clearly different water properties in this region (Itoh and Yasuda 2010) could explain the clear MLD differences (Fig. 2c). From 40°N to 45°N, clear differences were also evident between the distribution of MLDs in the anti-cyclonic and cyclonic eddies and between the MLDs inside and outside 100 km from anti-cyclonic eddy center (Fig. 2d), although there were not many available observations in this region.

In the composites (Fig. 2), deep MLDs were frequently observed within 125 km from the eddy centers. Assuming that 125 km was the scale within which eddies affected mixed-layer deepening, we calculated the proportions of the number of deep MLDs (>150 m) inside of the eddies (i.e., an observation within 125 km of an eddy core) to all observed deep MLDs in each grid box in the horizontal map (Fig. 3a) to estimate the contribution of the anti-cyclonic eddies to mixed-layer deepening. Furthermore, to take into account different frequencies of observed anti-cyclonic eddies in each box, we calculate temporal mean areas of the anti-cyclonic eddy within each box, and show the spatial distribution of the ratio of the number of observed deep MLDs per unit area within the anti-cyclonic

eddies to that in a whole box area (Fig. 3b). Note that 125 km is approximately double the typical eddy radius as estimated from the SSHA data (Itoh and Yasuda 2010). The typical radius of an eddy as defined using the Okubo–Weiss parameter encompasses the area where vorticity predominates over strain (i.e., only the inner part of the eddy core), and this radius is about half the radius of the entire vortex (Isern-Fontanet et al. 2006). The distance of 125 km used in this study probably corresponds to the radius of the entire vortex, which includes the areas with strong currents associated with the eddies. In addition, in this analysis, we also assume the frequencies of Argo float observations along the radial directions of the eddies were uniform, because the ratio of Argo float observations inside the anti-cyclonic eddies to all the observations was similar to that of the areas inside the eddies to all the areas (approx. 0.15).

Deep mixed layers were frequently observed from 140°E to 160°W (similar to the observations of Oka et al. 2011), and the contribution of anti-cyclonic eddies to the mixed-layer deepening, and thus to mode water formation, varied spatially (Fig. 3). In almost all the high-proportion areas in Fig. 3a, the ratios of the number of observed deep MLD per unit area were greater than unity (Fig. 3b). Thus, many deep MLDs were observed within anti-cyclonic eddies in the high-proportion areas (Fig. 3a) not just because of the presence of many eddies but also because of favorable conditions for deep MLDs associated with the anti-cyclonic eddies. As the areas with a high proportion of

Fig. 3 The proportion of the number of the deep mixed layers (>150 m) within 125 km of the center of anti-cyclonic eddies in all the observed deep mixed layers (a), and the ratio of the number of the deep mixed layers per unit area inside the anti-cyclonic eddies to that in a whole box (b). The proportion and ratio were calculated for each 5° × 2.5° box by using profile data from 2002 to 2009, and the total areas of the anti-cyclonic eddies were calculated assuming the radius of anti-cyclonic eddies was 125 km. Gray boxes had fewer than five observed deep mixed layers

(a) Proportion of the observed deep MLDs inside anti-cyclonic eddies

**(b)** Ratio of the numbers of deep MLDs per unit area inside anti-cyclonic eddies
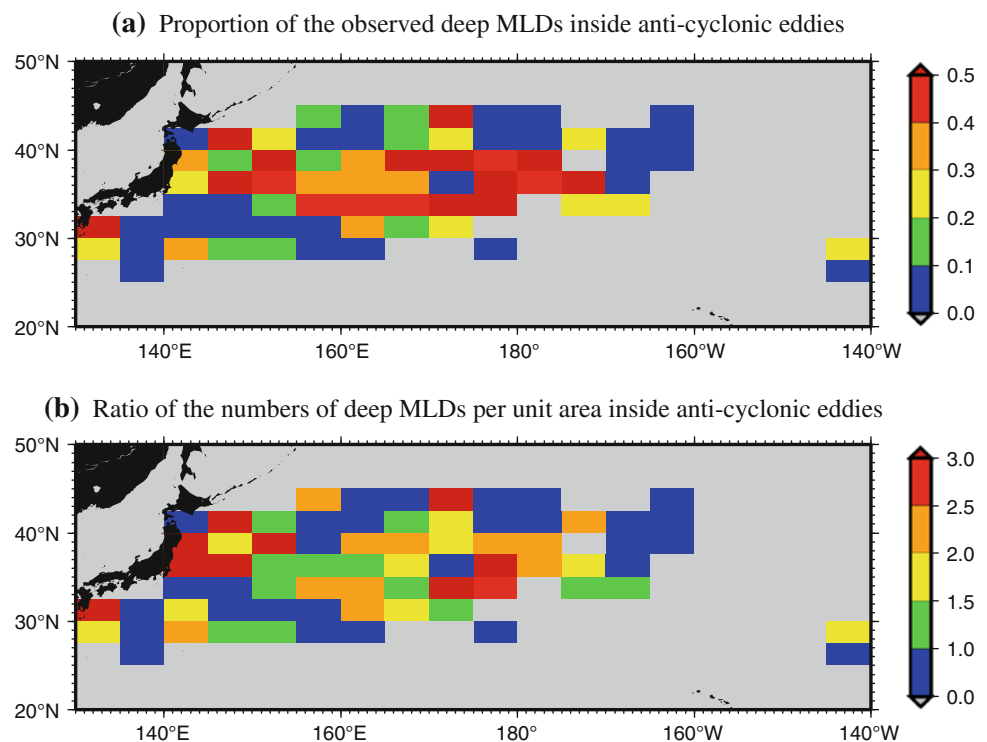
Table 2 Properties of mode waters around the inter-frontal zone in the North Pacific Ocean (adapted from Oka et al. 2011)

Type	Temperature (°C)	Salinity	Density (kg m^{-3})
STMW	16.0–21.5	34.65–34.95	24.2–25.6
L-CMW	10.0–16.0	34.30–34.65	25.4–26.3
D-CMW	8.0–10.5	33.80–34.20	26.1–26.5
TRMW	5.0–7.5	33.60–33.90	26.4–26.6

the number of deep MLDs within anti-cyclonic eddies were distributed in the region from 140°E to 160°W and from 35°N to 45°N (Fig. 3), the relationships evident in the composites (Fig. 2c) reflect the characteristics of a wide area with many eddies. There was also a high proportion of deep MLDs inside anti-cyclonic eddies around 35°N near the Kuroshio Extension, whereas the magnitude was relatively low around 30°N. North of 40°N, there are some regions where the proportion of the number of deep MLDs within anti-cyclonic eddies was high west of 160°E. This suggests that the relationships in the composites (Fig. 2d) reflect only a limited area mainly west of 160°E. The region with high proportion of the number of deep mixed layers inside anti-cyclonic eddies from 145°E to 160°E (Fig. 3) corresponded to the region along the quasi-stationary jet associated with the subarctic front (Isoguchi et al. 2006).

Oka et al. (2011) used the temperature and salinity relationships of mixed layers deeper than 150 m to classify water property in the deep mixed layers corresponding to mode water types, and described 4 mode water types (Table 2), because the deep mixed layers are the major source of mode waters in the North Pacific. In a similar manner, we grouped the observed deep MLDs (>150 m) by temperature and salinity characteristics and determined the proportion in each temperature-salinity bin that were distributed within anti-cyclonic eddies (Fig. 4). This grouping revealed four types of deep mixed layer waters similar to the 4 mode water types, separated by bins with fewer observations (4 rectangles surrounded white and gray boxes in Fig. 4). Note that deep MLDs were rarely observed in the cyclonic eddies (Fig. 2), and proportions of the number of deep MLDs within cyclonic eddies were less than 0.1 in almost all the temperature-salinity bins (not shown). Although deep mixed layers with the properties of STMW were not always observed in the anti-cyclonic eddies (Fig. 2b and around 30°N in Fig. 3), the relatively cold (<18°C) and fresh (<34.8) deep mixed layers in STMW (Fig. 4) were frequently found inside the anti-cyclonic eddies. Water similar to the colder and fresher range of STMW was often observed in the eastern part of the STMW formation region south of the Kuroshio Extension (Oka and Suga 2003), which suggests that the anti-cyclonic eddies contributed to the formation of
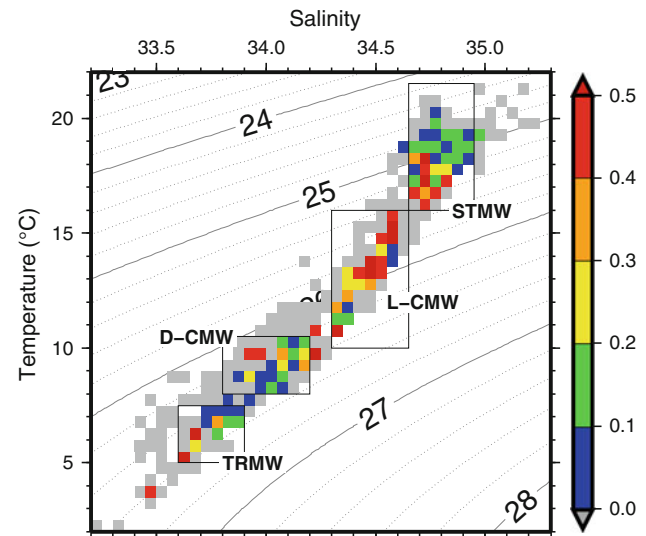

Fig. 4 Proportion of the number of deep mixed layers (>150 m) in the cores of anti-cyclonic eddies (<125 km) as a function of temperature and salinity. The *boxes* used for the summation were in increments of 0.5° for temperature and 0.05 for salinity. *Gray boxes* had fewer than five observed deep mixed layer. The four mode water types defined by Oka et al. (2011) (Table 2) are shown by *rectangles*

STMW, especially in the downstream region of the Kuroshio Extension, which is reflected in the high-proportion regions around 170°E and 35°N in Fig. 3. In contrast, the high proportions of the number of the deep mixed layers with the properties of L-CMW in the anti-cyclonic eddies (Fig. 4) reflected that the strong contribution of the anti-cyclonic eddies to deep mixed layers were detected broadly in the L-CMW formation area (Fig. 2c and from 35°N to 40°N in Fig. 3). As clearly defined large-scale fronts such as the Kuroshio Extension were not observed in the L-CMW formation region, the relatively weak preexisting stratification associated with the anti-cyclonic eddies could be more important there for mixed-layer deepening. There were smaller contributions from anti-cyclonic eddies to deep mixed layer formation in the D-CMW region, especially in its cold and fresh part, and relatively large contributions in the TRMW region (Fig. 4).

3.2 Contribution of sea-surface flux and preexisting stratification to mixed layer deepening

Because warmer (colder) water has frequently been observed in the cores of anti-cyclonic (cyclonic) eddies (Itoh and Yasuda 2010), we detected positive (negative) anomalies of bin-averaged sea surface temperature (SST), which were calculated from area-weighted averages within 350 km of the center of each eddy (Fig. 5). The differences between SST inside and outside eddies were larger north of the Kuroshio Extension (Fig. 5c, d) than south (Fig. 5a, b). In fact strong and large warm-core rings were reported north of

Fig. 5 Distribution of 50-km
bin averages of sea surface
temperature (SST) anomalies
(*blue curves*) and surface heat
(*red curves*) and momentum
(*green curves*) flux anomalies
from the ocean to the
atmosphere as a function of
distance from the center of
meso-scale eddies. The surface
temperature and flux anomalies
were calculated from area-
weighted averages within
350 km of the center of each
eddy. *Bars* denote bootstrapped
95% confidence intervals for bin
averages
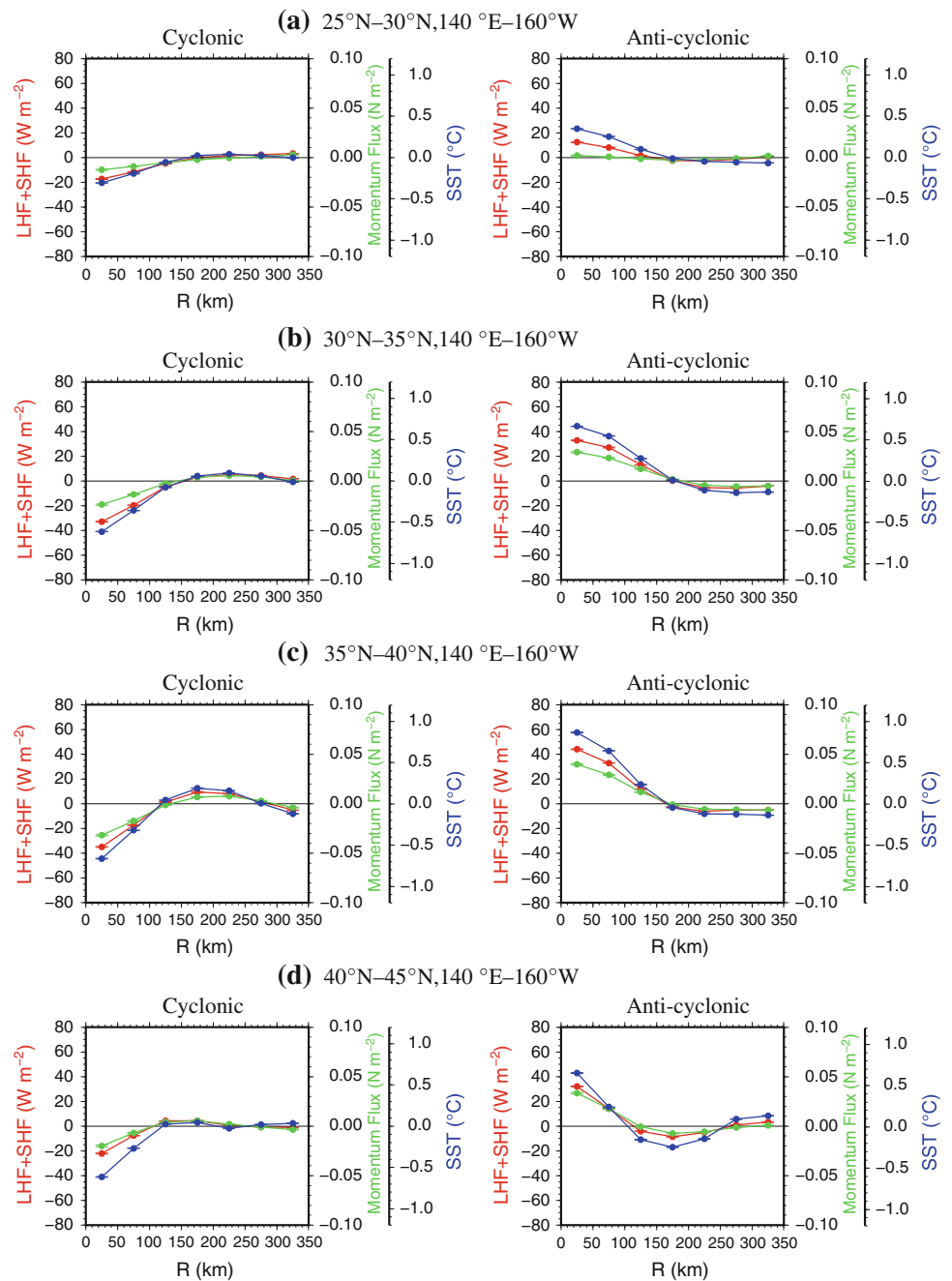
the Kuroshio Extension in previous studies, whereas such clear SST anomalies associated with meso-scale eddies were not frequently observed to the south (Mizuno and White 1983; Kawamura et al. 1986). This difference between the areas south and north of the Kuroshio Extension is reflected in the amplitude of composite SST anomalies in eddies.

The anomalies of both turbulent surface heat and momentum fluxes to the ocean, which were calculated from area-weighted averages within 350 km of the center of each eddy, associated with the SST anomalies in

eddies were positive (negative) in the core of anti-cyclonic (cyclonic) eddies (Fig. 5). The momentum flux anomalies reflect the tendency for wind near the ocean surface to be stronger over warmer water, as reported in previous studies (Nonaka and Xie 2003), and this relationship is also evident in the composite of the eddies detected from the SSHA (Fig. 5). Note that the 95% confidence intervals for bin-averaged anomalies of SST and surface fluxes were generally small, because of the large number of samples.

To evaluate the effects of the anomalies of turbulent heat and momentum fluxes (Fig. 5) and the preexisting stratification along a radial eddy section (Fig. 6) on the MLD distributions along a radial direction, we used the

bulk one-dimensional mixed layer model (Eq. 1). From 30°N to 35°N, the differences between observed MLDs inside and outside anti-cyclonic eddies were smaller than those for the cyclonic eddies (Fig. 7b). Because changes in

Fig. 6 Vertical temperature sections along the radial section of eddies averaged from October to December from 2002 to 2007 (°C). The contour intervals are 1°C
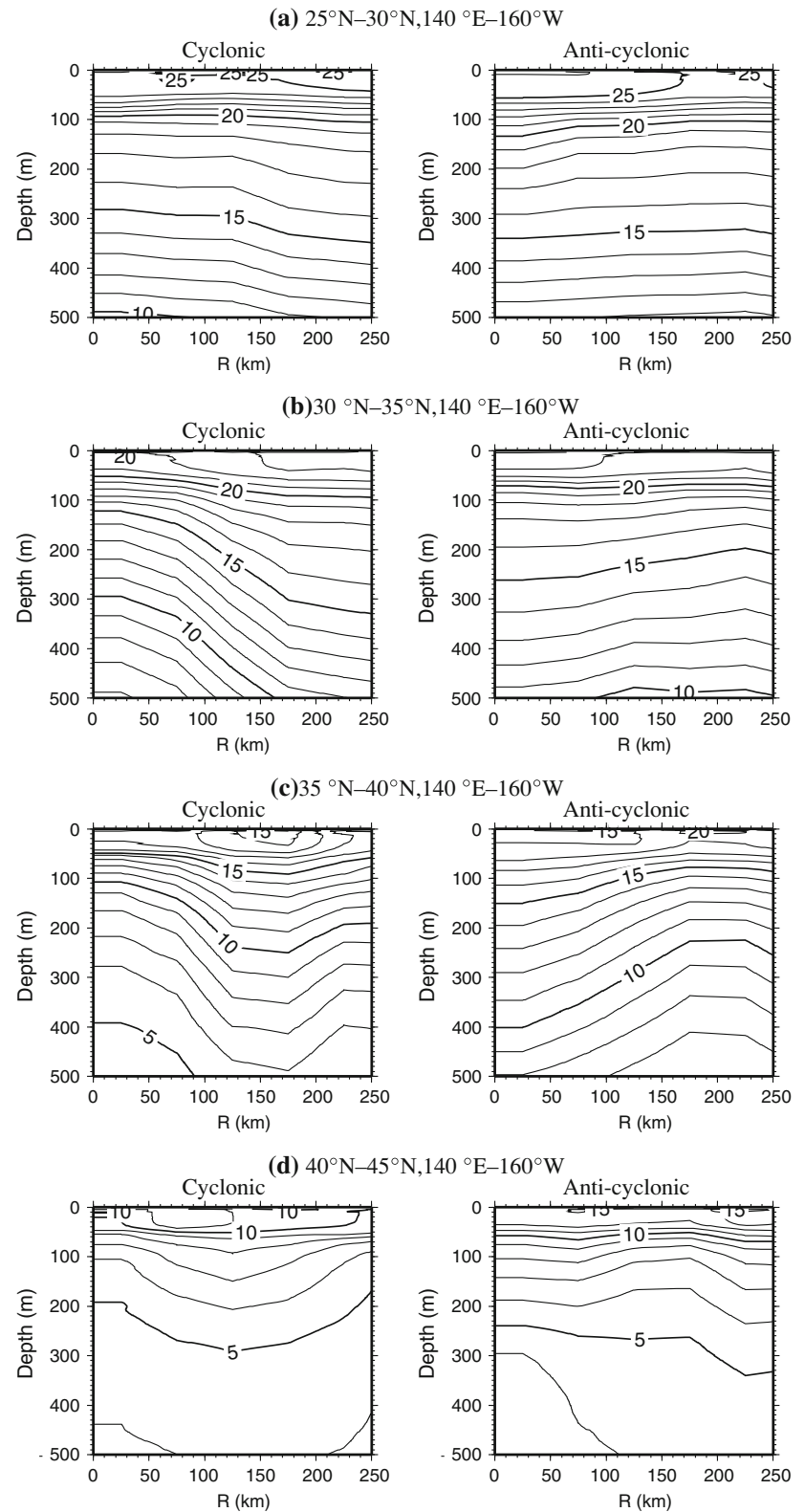
Fig. 7 Observed mixed layer depths (MLDs) and those estimated using the bulk mixed layer model as a function of distance along the radial direction of eddy. *White circles* denote the 50-km bin averages of observed MLDs similar to Fig. 2, but calculated using data from 2002 to 2007. *Green dots* denote MLDs estimated using the preexisting stratification associated with the eddies (Fig. 6) and a constant surface flux over the radial section, whereas *red dots* denote MLDs estimated using both the preexisting stratification and the surface flux associated with the eddies (Figs. 5, 6). *Bars* denote bootstrapped 95% confidence intervals for bin averages

(a) 25°N–30°N,140 °E–160°W

(b) 30°N–35°N,140 °E–160°W

(c) 35°N–40°N,140 °E–160°W

(d) 40°N–45°N,140 °E–160°W
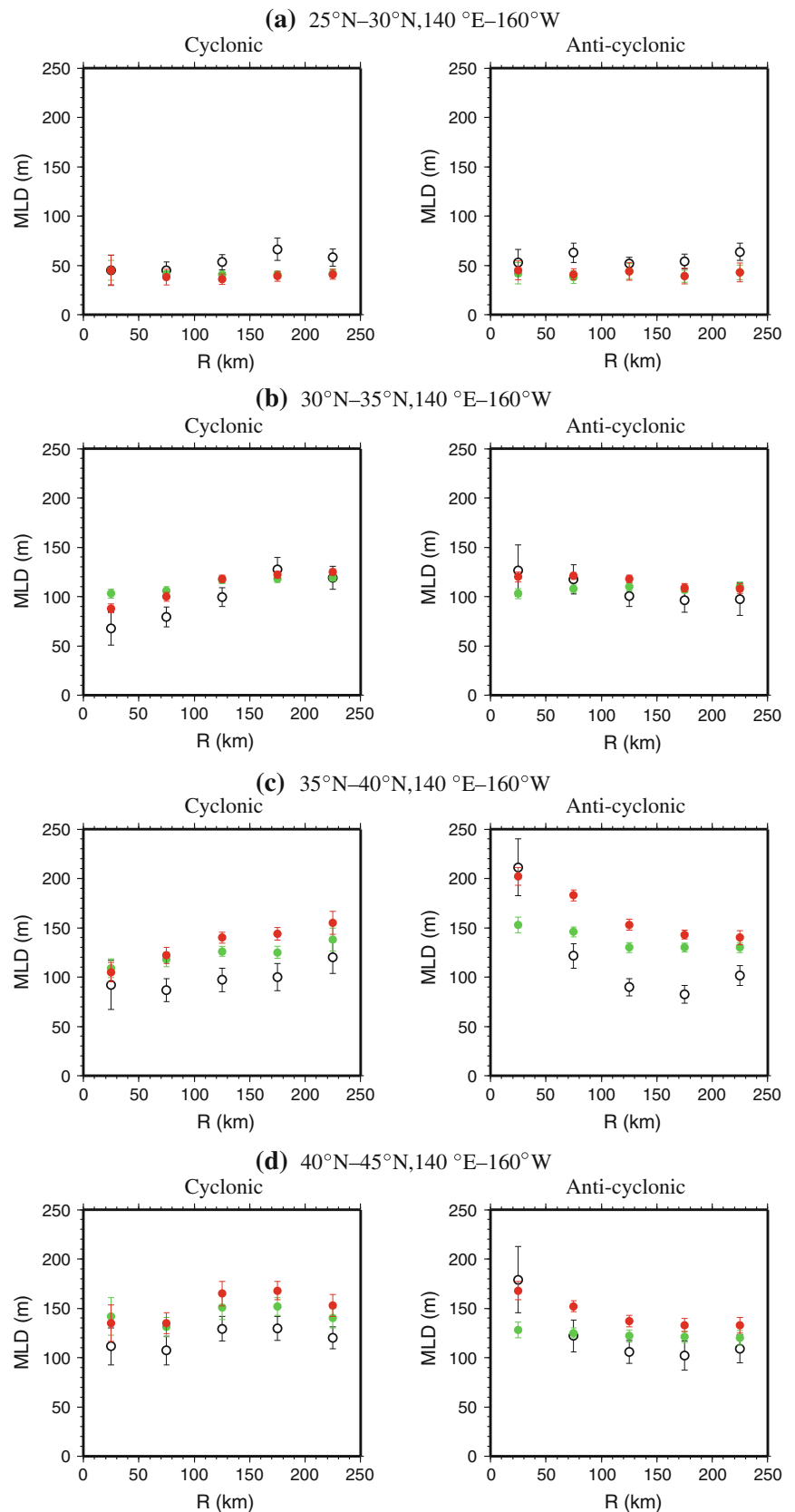
preexisting stratification along the radial section were larger in the cyclonic eddy than in the anti-cyclonic eddy (Fig. 6b), there were large differences between MLDs inside and outside the cyclonic eddies, estimated both with and without the surface flux distribution along the radial direction (green and red circles in Fig. 7b). On the other hand, MLDs of the anti-cyclonic eddies estimated without the surface flux anomalies change little along the radial direction (green circles in Fig. 7b). This difference is mainly because clearly defined cyclonic eddies are more frequently observed than anti-cyclonic eddies in this region (Itoh and Yasuda 2010).

In the region from 35°N to 40°N, both the flux anomaly and preexisting stratification changes along the radial directions (Figs. 5c, 6c) were obvious, and there were large changes of MLDs along the radial direction, which were estimated both with and without the surface flux distribution (Fig. 7c). Thus, both the flux anomaly and the preexisting stratification changes along the radial section strongly contributed to reproduction of the pattern changes in MLDs, although the difference of the estimated and observed MLDs was significantly large except within 50 km of the eddy centers (Fig. 7c). A large portion of the deep mixed layers observed in this region was located in the anti-cyclonic eddies (as discussed in the Sect. 3.1). Thus, the strong cooling and weak preexisting stratification inside the anti-cyclonic eddies are important in the formation of the deep mixed layers in this region, which contributed to the L-CMW source region.

The flux anomalies associated with the anti-cyclonic eddies were more important for forming the MLD changes in the radial direction than the preexisting stratification changes along the radial section in the region from 40°N to 45°N, because the MLD changes estimated using the surface flux distribution along the radial direction were clear, and those without the surface flux distribution were insignificant (Fig. 7d). As shown in the Sect. 3.1, deep mixed layers in anti-cyclonic eddies have frequently been observed near the east coast of Japan, where TRMW is formed; the flux anomalies associated with the eddies might be important for the formation of TRMW (Fig. 7d). As both the flux (Fig. 5a) and the preexisting stratification changes along the radial section (Fig. 6a) are small in the region of 25°N–30°N, the differences between MLDs inside and outside the eddies were small, and there were no clear differences between the estimated MLD distributions in the anti-cyclonic and cyclonic eddies (Fig. 7a).

4 Discussion

In this study, we have shown the relationships between deep mixed layers and spatial changes of ocean preexisting stratification and surface fluxes around the centers of meso-scale eddies detected by using satellite SSHA data in the western North Pacific Ocean, wherein the weak (strong) preexisting stratification and strong (weak) forcing inside the core of anti-cyclonic (cyclonic) eddies tend to foster the development of deep (shallow) mixed layers in the winter. These relationships were clear, especially in the inter-frontal zone between the Kuroshio Extension and subarctic front. This suggests that meso-scale eddies are important in forming mode waters in this area. The small-scale distribution of MLDs associated with the meso-scale eddies could affect the temporal variability of large-scale MLD through eddy activity variability, because decadal changes of eddy activity around the Kuroshio Extension were reported after use of SSHA observations and high-resolution numerical models (Qiu and Chen 2005; Taguchi et al. 2010). Because the heat and chemical constituents that are exchanged between the atmosphere and the ocean at the sea surface can be transported to the sub-surface layer in association with CMW subduction (Deser et al. 1996; Schneider et al. 1999; Emerson et al. 2004), the eddy activity around the inter-frontal zone might be involved in inter-annual climate variability. Furthermore, many studies have reported that the distribution of eddies in the inter-frontal zone corresponds to the sea surface color pattern (Saitoh et al. 1998); therefore the distribution of MLDs observed in this study could also affect the biological activity in the eddy cores.

The contributions of the anti-cyclonic eddies to form deep MLDs, which are important for mode water formation, were different spatially (Figs. 2, 3). In the STMW formation region, the changes in MLDs along the radial direction of anti-cyclonic eddies were relatively small (Fig. 2b), and there was a low proportion of the number of deep mixed layers inside the anti-cyclonic eddies around 30°N (Fig. 3). This is because both the relatively weak preexisting stratifications associated with anti-cyclonic eddies (near 35°N in Fig. 3) and those observed broadly south of the Kuroshio Extension (in the region of 30°N), because of the existence of STMW in the subsurface layer formed in previous winters, contribute to the formation of the deep mixed layers there. Furthermore, the small MLD changes along the radial direction of the anti-cyclonic eddies also reflected that the changes in surface flux and preexisting stratification along the radial directions were relatively small (Figs. 5b, 6b, 7b), mainly because of the presence of fewer clearly defined warm-core rings (Itoh and Yasuda 2010). In the L-CMW formation region that is not accompanied by clearly-defined large-scale fronts, for example the Kuroshio Extension, the relatively weak preexisting stratification associated with the anti-cyclonic eddies could be more important there for mixed-layer deepening. Thus, there was a clear MLD difference along

the radial direction of the anti-cyclonic eddy (Fig. 2c), because of the substantially different preexisting stratifications and surface fluxes along the radial direction (Figs. 5c, 6c, 7c), and large contribution of the anti-cyclonic eddies to deep MLDs were broadly detected spatially (Fig. 3) and in the temperature–salinity relationships (Fig. 4). The relatively strong contribution of anti-cyclonic eddies to deep mixed layers with the properties of TRMW (Fig. 4) might reflect that the anti-cyclonic eddies along the front (or ridges of the meander) were important for forming deep mixed layers with TRMW properties, as TRMW forms in the narrow area south of the subarctic front (Saito et al. 2007). Formation of TRMW west of 170°E and its subsequent eastward transportation are thought to set the precondition for formation and subduction of D-CMW east of 170°E (Oka et al. 2011). This might explain why there were fewer high-proportion bins with D-CMW properties in Fig. 4.

Some parts of thick homogeneous layers originating from the deep mixed layers in the anti-cyclonic eddies can be transported outside the eddies by eddy mixing, and be subducted into the permanent pycnocline by transportation along with isopycnal surfaces (Nishikawa et al. 2010). This process could contribute the broad distribution of mode waters in the permanent pycnocline. Other parts of the homogeneous layers seem to remain in the cores of mesoscale eddies during the sequential seasons. Furthermore, whereas some of these can also be subducted into the permanent pycnocline with the eddy moving (Nishikawa et al. 2010), the others remain under the seasonal pycnocline until the next winter, and can affect the deepening mixed layer. In the L-CMW formation area, while the many anti-cyclonic eddies are moving westward (Itoh and Yasuda 2010), the broad distribution of L-CMW in the main thermocline is observed in the downstream region of the interfrontal zone (Oka et al. 2011). The former process of eddy mixing and advections in the permanent pycnocline may contribute to the broad distribution of L-CMW in the permanent pycnocline near the downstream region, and the latter process of the thick homogeneous layer trapped in the cores may be dominant in the upstream regions, where the thick homogeneous layers were not broadly observed in the subsurface layer (Oka et al. 2011). However, these subduction processes around eddies were not directly shown in this study. To investigate the processes, we plan to investigate seasonal changes in the subsurface layers around eddies from future observations.

### 4.1 Dependency of criteria and large variances in composites

The results in this study were not strongly dependent on choices of criteria to determine MLDs (vertical density difference of 0.03 kg m^{-3}) and deep MLD (>150 m) with strong contributions to the formation of mode waters. Using the shallow (deep) criterion of 100 m (200 m) for deep MLDs, proportions of the number of deep MLDs in the anti-cyclonic eddies became only approximately 0.1 smaller (larger) than shown in this study. These changes were not very large, and the difference among the contributions of the anti-cyclonic eddies to mode waters shown in the temperature and salinity relationship were similar to Fig. 4 (not shown). Although MLDs defined with a large density difference criterion of (for example) 0.125 kg m^{-3} were approximately 40-m deeper than those shown in Fig. 1 (not shown), the proportions of the number of deep MLDs in the anti-cyclonic eddies became only about 0.1 smaller. This criterion choice for deep MLDs also did not strongly affect our results. Note that using such a large density-difference criterion, we might be able to avoid detecting many shallow mixed layers because of short-term warming in the early spring (e.g, approximately 10-m MLDs in Fig. 2), which might persist in the short-term and may cause underestimation of deep MLDs contributing to form mode waters, but the MLDs determined by this large density difference criterion tend to be overestimated because they include thermoclines in which water properties are not vertically homogeneous.

While we showed that the different MLDs and fluxes between in the anti-cyclonic and cyclonic eddies, and the changes along the radial directions of the eddies, were detectable in the 50-km bin averages with the bootstrapped confidence intervals, there were large variances in MLDs and fluxes (see dots in Fig. 2 for MLDs). Variance of eddy shapes (assuming axially symmetric shapes in this study) and uncertainty in the locations of eddy centers can cause such variances, and the large variances might be mainly due to short-term or more small-scale variability. Although warmer waters are much more frequently observed than colder waters in the anti-cyclonic eddies, anti-cyclonic eddies with cold waters, which are sometimes observed (Hosoda and Hanawa 2004; Itoh and Yasuda 2010), can also affect large variances of MLDs and SSTs. In the future, the phenomena causing such large variances will be described in detail by use of higher resolution SSH and long-term satellite SST observations.

In this study, the distribution of the MLDs along the radial direction of the eddies was reproduced by using the initial stratification and the surface flux distributions associated with the eddies through the bulk formula for the MLDs, although the variance of observed MLDs for each bin was large; this might be because of more small-scale or short-term variability. The effects of horizontal advection and diffusion, which were ignored in this study, are presumed to be small, because the model was integrated over winter only (for 4 months), and strong currents were unlikely to be

Fig. 8 Distribution of mixed layer depths (*left*) and anomalies of sea surface temperature and fluxes (*right*) along the radial direction of anti-cyclonic eddies in the upstream of 140°E–160°E (**a**) and the downstream of 160°E–180° (**b**) regions of the main L-CMW formation area (35°N–40°N). The *left* and *right* figures are same as Figs. 2 and 5 but for zonally narrow sub regions
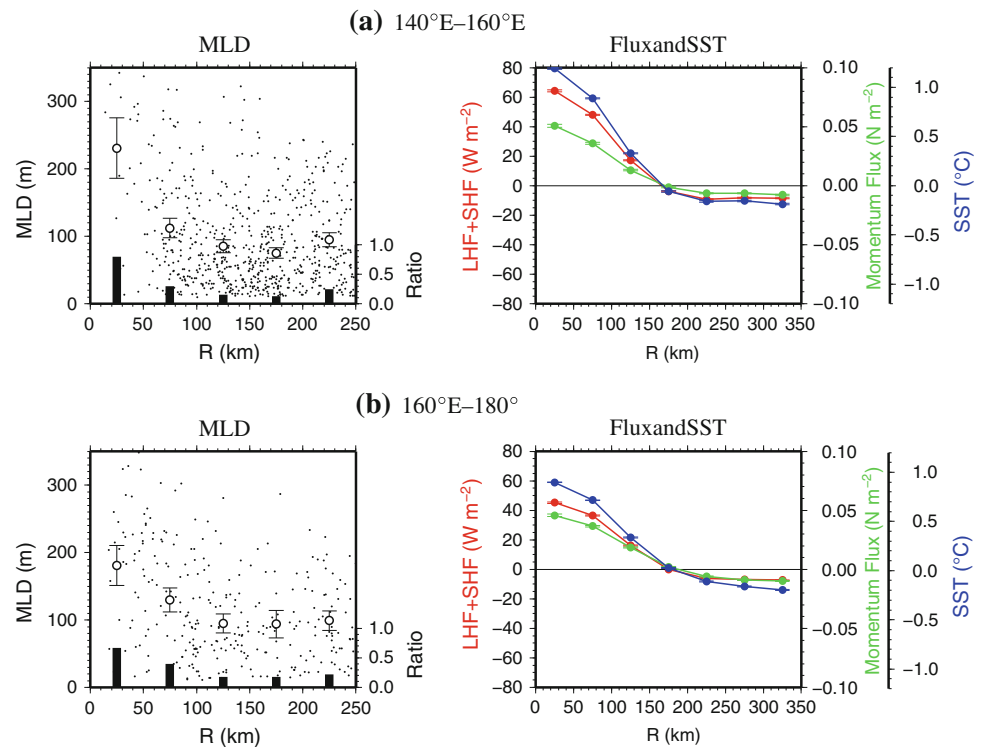
observed in the core of the eddies. However, there could be errors in the estimates because of the neglected effects, and the effect of horizontal advection might cause the difference between observed and estimated MLDs in Fig. 7.

The composites in this study were produced by using Argo float data, which provide intensive and uniform observations of ocean subsurface structure. However, more detailed observations (e.g., observations focusing on a eddy) are needed to clarify the processes causing deepening of mixed layers and formation of mode waters in eddies, taking into account horizontal advection. Furthermore, although we showed there were some spatial changes in relationships between meso-scale eddies and deep mixed layers, by showing the proportions of the number of deep MLDs inside the anti-cyclonic eddies in the 5° × 2.5° boxes (Fig. 3), available observations are not yet sufficient to enable description of detailed spatial changes in the relationships. For example, along the radial directions of the anti-cyclonic eddy, there were the differences of MLDs and flux anomalies between in the upstream (western) and downstream (eastern) regions of the L-CMW formation area (Fig. 8). The larger flux anomalies in the anti-cyclonic eddies might cause the deeper MLDs in the upstream region than in the downstream region, and this suggested that flux anomalies corresponding to the meso-scale eddy were more important in the upstream regions. However, it was difficult to determine preexisting stratification structures along the radial sections (similar to Fig. 6) because of the small number of available

observations in these small sub-regions. It is also difficult to describe relationships among the inter-annual subsurface temperature changes, eddy activity, and the process of mode waters subduction, because intense observations by Argo floats have only been carried out for approximately 5 years in the North Pacific. Continued and more intense observations by use of Argo floats, fine scale observations by ships and gliders, and analysis with high-resolution numerical models should help clarify the temporal and spatial changes in detail.

References

Akima H (1970) A new method of interpolation and smooth curve fitting based on local procedures. J Assoc Comput Mach 17:589–603

Chelton DB, Schlax MC, Samelson RM, de Szoeke RA (2007) Global observations of large oceanic eddies. Geophys Res Lett 34:L15606. doi:10.1029/2007GL030812

de Boyer Montégut C, Madec G, Fischer AS, Lazar A, Iudicone D (2004) Mixed layer depth over the global ocean: an examination of profile data and a profile-based climatology. J Geophys Res 109:C12,003

Deser C, Alexander MA, Timlin MS (1996) Upper-ocean thermal variations in the North Pacific during 1970–1991. J Climate 9:1840–1855

Emerson S, Watanabe YW, Ono T, Mecking S (2004) Temporal trends in apparent oxygen utilization in the upper pycnocline of the North Pacific: 1980–2000. J Oceanogr 60:139–147

Gu D, Philander SGH (1997) Interdecadal climate fluctuations that depend on exchanges between the tropics and extratropics. Sci Agric 275(5301):805

Hanawa K, Sugimoto S (2004) 'Reemergence' areas of winter sea surface temperature anomalies in the world's oceans. Geophys Res Lett 31:l10303. doi:10.1029/2004GL019904

Hanawa K, Talley LD (2001) Mode waters. In: Siedler G, Church J, Gould J (eds) Ocean circulation and climate. Academic Press, San Diego, pp 373–386

Hosoda K, Hanawa K (2004) Anticyclonic eddy revealing low sea surface temperature in the sea south of Japan: case study of the eddy observed in 1999–2000. J Oceanogr 60(4):663–671

Hosoda S, Ohira T, Sato K, Suga T (2010) Improved description of global mixed-layer depth using Argo profiling floats. J Oceanogr 66:773–787

Isern-Fontanet J, Font J, García-Ladona E, Emelianov M, Millot C, Taupier-Letage I (2004) Spatial structure of anticyclonic eddies in the Algerian basin (Mediterranean Sea) analyzed using the Okubo–Weiss parameter. Deep Sea Res II 51(25–26):3009–3028

Isern-Fontanet J, García-Ladona E, Font J (2006) Vortices of the Mediterranean Sea: an altimetric perspective. J Phys Oceanogr 36(1):87–103

Isoguchi O, Kawamura H, Oka E (2006) Quasi-stationary jets transporting surface warm waters across the transition zone between the subtropical and the subarctic gyres in the North Pacific. J Geophys Res 111(C10):C10,003

Itoh S, Yasuda I (2010) Characteristics of mesoscale eddies in the Kuroshio–Oyashio extension region detected from the distribution of the sea surface height anomaly. J Phys Oceanogr 40:1018–1034

Itoh S, Yasuda I (2010) Water mass structure of warm and cold anticyclonic eddies in the western boundary region of the subarctic North Pacific. J Phys Oceanogr 40:2624–2642

Kako S, Kubota M (2009) Numerical study on the variability of mixed layer temperature in the North Pacific. J Phys Oceanogr 39(3):737–752

Kalnay E, Kanamitsu M, Kistler R, Collins W, Deaven D, Gandin L, Iredell M, Saha S, White G, Woollen J, Zhu Y, Leetmaa A, Reynolds R, Chelliah M, Ebisuzaki W, Higgins W, Janowiak J, Mo KC, Ropelewski C, Wang J, Jenne R, Joseph D (1996) The NCEP/NCAR 40-year reanalysis project. Bull Am Meteor Soc 77(3):437–471

Kawamura H, Mizuno K, Toba Y (1986) Formation process of a warm-core ring in the Kuroshio–Oyashio frontal zone–December 1981–October 1982. Deep Sea Res A 33(11–12):1617–1640

Latif M, Barnett TP (1994) Causes of decadal climate variability over the North Pacific and North America. Sci Agric 266(5185):634

Masuzawa J (1969) Subtropical mode water. Deep Sea Res 16:453–472

Minobe S, Kuwano-Yoshida A, Komori N, Xie S, Small R (2008) Influence of the Gulf Stream on the troposphere. Nat Biotechnol 452(7184):206–209

Mizuno K, White W (1983) Annual and interannual variability in the Kuroshio current system. J Phys Oceanogr 13:1847–1867

Nakamura H (1996) A pycnostad on the bottom of the ventilated portion in the central subtropical North Pacific: its distribution and formation. J Oceanogr 52(2):171–188

Nishikawa S, Tsujino H, Sakamoto K, Nakano H (2010) Effects of mesoscale eddies on subduction and distribution of Subtropical Mode Water in an eddy-resolving OGCM of the western North Pacific. J Phys Oceanogr 40:1748–1765. doi:10.1175/2010JPO4261.1

Nonaka M, Xie SP (2003) Covariations of sea surface temperature and wind over the Kuroshio and its extension: evidence for ocean-to-atmosphere feedback. J Climate 16:1404–1413

Ohno Y, Iwasaka N, Kobashi F, Sato Y (2009) Mixed layer depth climatology of the North Pacific based on Argo observations. J Oceanogr 65(1):1–16

Oka E (2009) Seasonal and interannual variation of North Pacific subtropical mode water in 2003–2006. J Oceanogr 65(2):151–164

Oka E, Suga T (2003) Formation region of North Pacific subtropical mode water in the late winter of 2003. Geophys Res Lett 30(23):2205. doi:10.1029/2003GL018581

Oka E, Suga T (2005) Differential formation and circulation of North Pacific central mode water. J Phys Oceanogr 35(11):1997–2011

Oka E, Talley LD, Suga T (2007) Temporal variability of winter mixed layer in the mid-to high-latitude North Pacific. J Oceanogr 63(2):293–307

Oka E, Kouketsu S, Toyama K, Uehara K, Kobayashi T, Hosoda S, Suga T (2011) Formation and subduction of central mode water based on profiling float data, 2003–2008. J Phys Oceanogr. 41:113–129. doi:10.1175/2010JPO4419.1

Qiu B, Chen S (2005) Variability of the Kuroshio extension jet, recirculation gyre, and mesoscale eddies on decadal time scales. J Phys Oceanogr 35(11):2090–2103

Qiu B, Hacker P, Chen S, Donohue KA, Watts DR, Mitsudera H, Hogg NG, Jayne SR (2006) Observations of the subtropical mode water evolution from the Kuroshio extension system study. J Phys Oceanogr 36(3):457–473

Rainville L, Jayne SR, McClean JL, Maltrud ME (2007) Formation of subtropical mode water in a high-resolution ocean simulation of the Kuroshio extension region. Ocean Model 17(4):338–356

Roemmich D (2001) Observing the Oceans in the 21st Century, Bureau of Meteorology. In: Argo: the global array of profiling floats, pp 248–258

Saito H, Suga T, Hanawa K, Watanabe T (2007) New type of pycnostad in the western subtropical-subarctic transition region of the North Pacific: transition region mode water. J Oceanogr 63(4):589–600

Saitoh SI, Inagake D, Sasaoka K, Ishizaka J, Nakame Y, Saino T (1998) Satellite and ship observations of Kuroshio warm-core ring 93A off Sanriku, northwestern North Pacific, in spring 1997. J Oceanogr 54(5):495–508

Schneider N, Miller AJ, Alexander MA, Deser C (1999) Subduction of decadal North Pacific temperature anomalies: observations and dynamics. J Phys Oceanogr 29(5):1056–1070

Suga T, Takei Y, Hanawa K (1997) Thermostad distribution in the North Pacific subtropical gyre: the central mode water and the subtropical mode water. J Phys Oceanogr 27(1):140–152

Suga T, Motoki K, Aoki Y, Macdonald A (2004) The North Pacific climatology of winter mixed layer and mode waters. J Phys Oceanogr 34(1):3–22

Sugimoto S, Hanawa K (2005) Remote reemergence areas of winter sea surface temperature anomalies in the North Pacific. Geophys Res Lett 32(1):L01606. doi:10.1029/2004GL021410

Taguchi B, Qiu B, Nonaka M, Sasaki H, Xie S, Schneider N (2010) Decadal variability of the Kuroshio extension: mesoscale eddies and recirculation. Ocean Dyn 60:673–691

Takahashi T, Sutherland SC, Wanninkhof R, Sweeney C, Feely RA, Chipman DW, Hales B, Friederich G, Chavez F, Sabine C, Watson A, Bakker DCE, Schuster U, Metzl N, Yoshikawa-Inoue H, Ishii M, Midorikawa T, Nojiri Y, Körtzinger A, Steinhoff T, Hoppema M, Olafsson J, Arnarson TS, Tilbrook B, Johannessen T, Olsen A, R B, Wong CS, Delille B, Bates NR, de Baar HJW (2009) Climatological mean and decadal change in surface ocean pCO$_2$, and net sea-air CO$_2$ flux over the global oceans. Deep Sea Res II 56(8–10):554–577

Talley LD, Raymer ME (1982) Eighteen degree water variability. J Mar Res 40:757–775

Tatebe H, Yasuda I (2001) Seasonal axis migration of the upstream Kuroshio extension associated with standing oscillations. J Geophys Res 106:16,685–16,692

Tokinaga H, Tanimoto Y, Nonaka M, Taguchi B, Fukamachi T, Xie S, Nakamura H, Watanabe T, Yasuda I (2006) Atmospheric sounding over the winter Kuroshio extension: effect of surface stability on atmospheric boundary layer structure. Geophys Res Lett 33(4)

Tokinaga H, Tanimoto Y, Xie S, Sampe T, Tomita H, Ichikawa H (2010) Ocean frontal effects on the vertical development of clouds over the western North Pacific: In situ and satellite observations. J Climate 22:4241–4260

Tomita H, Kubota M, Cronin M, Iwasaki S, Konda M, Ichikawa H (2010) An assessment of surface heat fluxes from J-OFURO2 at the KEO and JKEO sites. J Geophys Res 115(C3):C03,018

Toyama K, Suga T (2010) Vertical structure of North Pacific mode waters. Deep Sea Res II 57:1152–1160

Tsujino H, Yasuda T (2004) Formation and circulation of mode waters of the North Pacific in a high-resolution GCM. J Phys Oceanogr 34(2):399–415

Uehara H, Suga T, Hanawa K, Shikama N (2003) A role of eddies in formation and transport of North Pacific subtropical mode water. Geophys Res Lett 30(13):1705

Von Storch H, Zwiers FW (1999) Statistical Analysis in Climate Research. Cambridge University Press, Cambridge

Weller RA, Plueddemann AJ (1996) Observations of the vertical structure of the oceanic boundary layer. J Geophys Res 101(C4):8789–8806

White WB, Annis JL (2003) Coupling of extratropical mesoscale eddies in the ocean to westerly winds in the atmospheric boundary layer. J Phys Oceanogr 33(5):1095–1107

Wong A, Keeley R, Carval T, Argo Data Management Team (2010) Argo quality control manual. Argo Data Management Team, version 2.5 edn, available from web site of Argo Data Management, http://www.argodatamgt.org/

Yasuda I, Tozuka T, Noto M, Kouketsu S (2000) Heat balance and regime shifts of the mixed layer in the Kuroshio Extension. Prog Oceanogr 47:257–278